Apr 1st, 8:00 AM

Communication Channel Model of the Atmosphere for Optical Frequencies

Eli Brookner
Information Theory Section

Raytheon Company
Space and Information Systems Division

COMMUNICATION CHANNEL MODEL OF THE ATMOSPHERE FOR OPTICAL FREQUENCIES

By
Dr. Eli Brookner
Manager, Information Theory Section

Raytheon Company
Space and Information Systems Division
Sudbury, Massachusetts

Abstract

In order to obtain high data rate T.V. picture transmissions from spacecrafts on planetary missions consideration has been given in the past to the use of laser communications systems. If no relay satellite is used a deep space laser communication link would involve propagation through the earths atmosphere to a ground based station. This paper gives consideration to the characteristic of the earths atmosphere as a communication channel. A channel model is given both for clear weather conditions and for inclement weather conditions. For clear weather conditions it is found that the laser atmosphere is a Quasi-Wide-Sense-Stationary correlated Scattering Channel (QWSSCS) which can be fairly accurately characterized by an array of variable gain, variable delay paths. Under inclement weather conditions the channel is characterized by a differential circuit model which is specified by the Input Delay-Spread Function. Data is compiled, for these two channel models, which describes the pertinent parameters, such as, delay dispersion, the amplitude distribution, amplitude power spectrum and the two dimentional spacial correlation function. It is found that for good weather conditions, pulses having widths of the order of 2 picosecond can be propagated through the whole atmosphere without appreciable distortion, whereas for inclement weather conditions one is limited to pulse widths of the order of nanoseconds.

1. Clear Weather Model

First consideration is given to the channel coherent bandwidth limitations resulting from delay dispersion.

In the laser channel dispersion can arise from two factors. One of these factors is dispersion arising from multiple propagation paths while the other arises from the structural resonances of the molecules of the atmosphere which give rise to index of refraction variations with frequency and to absorption lines.

The laser signal multipath ray structure comes about from a number of phenomena. Multipaths can arise from atmospheric refraction, scattering from atmospheric turbulence, and scattering from particles in the atmosphere. In clear weather, i.e., for conditions where there is no rain, fog, snow, sleet, or hail present, the contribution from particle scattering is small. Hence only the effects of atmospheric refraction and scattering from atmospheric turbulences need be considered. The multipaths arising from these phenomena will be present when the receiving aperture is small as well as when it is large. Figure 1 shows the scattering paths arising from atmospheric refraction and turbulence. The figure shows how two rays, rays 1 and 2, will be received by one smaller region of the receiving aperture so that multipathing can exist for a small aperture receiver.

It is apparent from Figure 1 that the number of multipaths will increase as the area of the receiving dish is increased if the transmitted beam is wider than the receiving aperture. In this case one has multipathing due to the fact that different rays arriving at widely different points on the aperture see different atmospheric inhomogeneities. In particular, in Figure 1, ray 1 sees a completely different atmospheric inhomogeneity than ray 5. As a result the propagation properties for ray 1 are different than those for ray 5. Moreover, the amplitude and phase of the signal received due to ray 1 will be different from that due to rays 5 and 6.

The ensuing arguments indicate that for ground receiver apertures less than 6 meters in diameter, the channel distortion to pulse transmission is primarily determined by molecular structural resonances when weak or moderate turbulent atmospheric conditions prevail while for strong turbulence conditions the pulse spreading contributed by multipathing approximately equals that due to the delay dispersion resulting from atmosphere index of refraction variations with frequency. It is shown that multipath-pulsewidth spreading present with small apertures as a result of paths such as 1 and 2 of Figure 1 is completely negligible (being of the order of 0.01 picosecond or less in some cases), whereas the multipath-pulsewidth spreading arising from paths such as 1 and 5 for a large aperture can be expected to be generally smaller than those due to molecular resonances except when one has strong turbulence conditions.

The multipathing arising for a small aperture (less than 1 mm in diameter) shall now be considered. Muchmore and Wheelan carried out a theoretical analysis indicating that the multipathing that would be exhibited for a small ground receiver aperture is of no consequence.[1] Their analysis indicates that if the coherent bandwidth were

limited by multipathing for a small aperture, the coherent bandwidth would be over 10% of the carrier frequency at or near the visible region of the spectrum. In their analysis they use a first order Born approximation. Their conclusions appear to be backed up by experimental star data obtained during good seeing conditions. Observations of the star Sirius with a 5-inch aperture have indicated flat fading of the received light signal over a 1,000 Å bandwidth in the visible spectrum.[2,3] 1000 Å corresponds to a bandwidth of 1.3×10^{14} Hz for $\lambda = 0.5$ μm which is equivalent to a fractional bandwidth of about 20%. It follows that the maximum difference in propagation time for two rays reaching a common point on a receiver aperture (as rays "1" and "2" in Figure 1) will be about 0.01 picosec.

Consideration is now given to the multipathing and dispersion that arises when one has a large ground receiver aperture. First, it follows from the above theoretical results and experimental star fading results that the multiple ray paths obtained for one frequency will be the same as those obtained for another frequency. That is, the multiple ray structure is essentially independent of the laser frequency. This will be true for frequency bands considerably larger than those of interest for communication. Furthermore, from the above theoretical and experimental data it follows that for the large aperture case the dispersion arising from multipathing will be due to the differences in the propagation times from the transmitter to different points on the receiver aperture. The multipathing coherence bandwidth will be determined by the largest difference that exists in the propagation time for two such paths. For strong atmospheric turbulence and a ground receiver aperture size of about 6 meter one can expect an average dispersion due to multipathing to be of the order of about 0.6 picosec. when the propagation path is through the whole atmosphere with the path having an elevation angle of 20°. For strong turbulence conditions and a vertical path through the atmosphere the dispersion due to multipathing is expected to be about 0.4 picosec. for a 6 meter receiver aperture.

Let us arbitrarily define the channel coherence bandwidth as one over the pulse width for which the channel produces 30% pulse width broadening. Then the above results indicate that if multipathing was the only factor giving rise to channel dispersion the coherence bandwidth would be 3×10^{13} Hz at $\lambda = 0.5$ μm for the case of a small aperture while for strong turbulence conditions and a large receiving aperture of 6 m diameter the coherence bandwidth would be about 5×10^{11} Hz for a path having a 20° elevation angle and about 8×10^{11} Hz for a vertical path. However, as stated previously pulse spreading arises in the channel also from molecular resonances in the atmosphere. Attention is now given to the effects of molecular structural resonances.

Consider the index of refraction variations in the visible region at the ruby wavelength of 6943 Å. Born and Wolf[4] present data which indicate that the index of refraction variation with wavelengths in the region of the wavelength 6943 Å is 1.5×10^{-9} parts per Å. For this slope of the index of refraction variation with wavelength, a 1.7 picosecond Guassianly shaped pulse when transmitted vertically through the whole atmosphere will have its pulse width increased by 30% or equivalently 0.5 picosec.[5] Thus one has for this case a coherence bandwidth of about 6×10^{11} Hz (4Å).

The coherence bandwidth will decrease with decreasing line-of-sight elevation angles in inverse proportion to the square root of the equivalent distance of atmosphere propagated through. Thus for an elevation angle of 20° the coherence bandwidth of the atmospheric channel will decrease about 40% to about 4×10^{11} Hz (2.5 Å). The coherence bandwidth will also change with the carrier frequency. The results given by Born and Wolf[4] indicate that the coherence bandwidth available for propagation vertically through the atmosphere decreases with increasing frequency reaching a value of 2.5×10^{11} Hz at the ultraviolet wavelength of 0.3 μm.

In contrast, from the previous calculations, the coherence bandwidth available from multipathing effects alone is 8×10^{11} Hz when propagating vertically through the atmosphere with strong turbulence existing and with a 6 meter receiver dish being used on the ground. If the atmospheric turbulence is moderate, the coherence bandwidth for this case will increase to about 24×10^{12} Hz.

It follows from the above that the dispersive effects due to multipathing when strong atmospheric turbulence exists and a 6 meter receiver aperture is used approximately equals the dispersive effects due to index of refraction variations at the ruby carrier wavelength of 6943 Å and will be smaller when medium or weak turbulence exists. Also at the wavelength of 0.3 μm the index of refraction effects dominate even for strong turbulence conditions. In all cases the multipath dispersion effects that exist for small collecting apertures are of no consequence.

In the above discussion only the part of the possible pulse distortion brought about by molecular structural resonances because of the index of refraction variations they introduce was taken into account. Molecular structural resonances can also bring about pulse distortion because of the absorption lines they produce. The possible degrading effects of these resonances shall now be dealt with.

Figure 2 shows the absorption lines observed in the tuneable range of radiation wavelengths for the ruby laser.[6] The ruby laser operating temperatures which give the wavelengths indicated along the

abscissa are given by a separate abscissa in the figure. The results given in the figure are for percent absorption when transmitting through the entire atmosphere at an elevation angle of about 18°. The intensities of the absorption lines shown will decrease appreciably for propagation vertically through the atmosphere instead of at an elevation angle of 18°. For example, a line giving 65% absorption for an 18° elevation angle results in only 25% absorption for a vertical propagation path.

The delay dispersion resulting from any of the absorption lines shown by itself is negligible even at the center of the absorption lines. For example the change of the index of refraction with wavelength at the center of the H_2O line at 6943.8 Å for the elevation angle of 18° is estimated to be only 0.4×10^{-9} parts per Å as compared to the value of 1.5×10^{-9} parts per Å obtained previously from Born and Wolf's data. (The H_2O 6943.8 Å line results are based on the fact that for a path through the atmosphere at an elevation angle of 18° the absorption at this wavelength is about 65% typically while the half-line width is about 0.064 Å.)[6] However, it is apparent that if a signal having a bandwidth of 0.12 Å (8×10^9 Hz) where transmitted using a wavelength of 6943.86 Å then only half the signal would be transmitted. Thus if 0.12 nanosecond pulses were transmitted at the wavelength of 6943.86 Å through the whole atmosphere at the elevation angle of 18°, the received pulses would be spread out to a width of about 0.24 nanosecond. The received pulses would also have about half the energy they would have if propagated at the wavelength of let us say 6943 Å for example. Figure 2 indicates that the maximum coherence bandwidths available which are free from bands of attenuation are equal to the separation between absorption lines. For example, for the ruby laser operated at 300°c this coherence bandwidth would be about 0.4 Å or 10^{11} Hz under good weather conditions when propagation takes place through the whole atmosphere at an elevation angle of the order of eighteen degrees.

It should be emphasized that in spite of the absorption lines shown in Figure 2, the above results indicate that one should be able to transmit through the whole atmosphere, at an elevation of 20°, Guassian shaped pulses having a width of about 2.5 picoseconds with reasonable fidelity at ruby laser wavelengths under conditions of weak or moderate turbulence.

Figure 3 shows the absorption lines observed near the gallium arsenide, GaAs, wavelength of 8446.2 Å when propagating through the whole atmosphere.[7] The figure indicates no atmospheric absorption lines near the laser wavelength. The nearest absorption line, a very weak one, is about 1 Å away. Thus the coherence bandwidth free of absorption lines appears to be wider at the GaAs wavelength than indicated above for the ruby wavelength. A similar curve to that of Figure 2 and 3 given for near the neon laser wavelength of 6328.2 Å indicates that the coherence bandwidth free of absorption lines that is available at this wavelength is about 0.8 Å. For a rather extensive listing and discussion of the atmospheric resonance lines near other laser frequency in the range from 0.6 μm to 18.6 μm see Reference (7).

It should be pointed out that no short pulse experimental measurements have been carried out to determine the shortest pulses that can be transmitted through the atmosphere. Short pulse propagation measurements made, though, over a path length of 1.8 miles using a GaAs diode laser source indicates that the coherent bandwidth is over 500 MHz under good weather conditions.[8]

One can conclude from the above that under clear weather conditions the coherence bandwidth, free of absorption lines, for the laser link may be 100 GHz or greater for a properly chosen laser frequency. It is apparent from the above that neither dispersion due to index of refraction variation with frequency or large aperture multipathing dispersion will limit the coherence bandwidth of a laser communication system in the near future for the bandwidths being contemplated. The large aperture dispersion does, however, effect the size of the aperture over which the signal can be coherently integrated for a heterodyning system.

It is now possible to specify the equivalent circuit for the optical communications channel. The channel is here characterized between the transmitting aperture and a specified receiving aperture. The receiving area and shape can be arbitrary but is here assumed to be in a plane perpendicular to the mean propagation path. The processing over the receiving aperture is left unspecified.

It follows from the above that the equivalent circuit for the optical communication channel can be represented as shown in Figure 4. The figure shows that it consists of a passive, non-time varying filter, followed by a parallel combination of frequency independent delay lines. Each delay line path has in it an amplifier which has a time variable gain. Each delay time path in the figure represents an equivalent circuit for the scatter path from the transmitter to a small element receiving area on the receiving aperture. (Although there exists in actuality more than one path between the transmitter and any point on the receiver, see Figure 1, because of the small difference in delay between these paths they may for all practical purposes be considered as one path.) The amplitude and phase characteristics of the passive network $H(w)$ corresponds to the amplitude and phase characteristics arising from the atmosphere molecule structural resonances.

For a particular scatter path the gain of the amplifier is given by $G(x,y,t)dxdy$ where $G(x,y,t)$ is a time variable gain function with x and y indicating the position of the elemental receiver area corresponding to the scatter path in question in terms of orthogonal corrdinates defined over the receiver aperture and with time being expressed by the variable t. The product dxdy represents the elemental receiving area for the

scatter path. The delays for each of the delay lines corresponding to the different paths are not constant but instead are random functions of time also. The time delay for a particular path is given by the time variable delay function $\tau(x, y, t)$.

The amplitude and time of arrival for the signal received over a small receiving aperture will not be a stationary variable if observed over a very long time (a whole day, for example). However, when observed over a short time (a quarter-of-an-hour, for example) the observables will, in general, be stationary and thus the system can be considered quasi-stationary. One has in effect a Quasi-Wide-Sense Stationary Correlated Scattering Channel (QWSSCS).[9]

When observed over a reasonably short time the amplitude of the signal received over a small aperture has a log normal distribution. Hence, the gains of the amplifiers in each of the paths shown in Figure 4, are log normally distributed. That is, the amplifier gain, G, has a probability density distribution given by:

$$P(G) = \frac{1}{\sqrt{2\pi}\,|G|\,\sigma_1} \exp - \frac{(\ln G)^2}{2\,\sigma_1^2} \qquad (1)$$

where σ_1^2 is the variance of the natural logarithm of G, i.e. of ln G.

Table 1 tabulates for the assumption of plane-wave propagation the variance, σ_1^2, of $\ln G/G_o$, where G_o is the scatter path gain under the assumption of no refractive index variations. Also given in the table is the variance of G, σ_G^2, and the mean of G, $G = m_G$.

The results in Table 1 are given for two wavelengths $\lambda = 0.63$ μm and 10.6 μm and for several propagation paths: a 1 km path 50 meters above the earths surface, a 15 km path 50 meters above the earths surface, and a path through the total atmosphere. For the horizontal paths the inner scale size l_o was taken to be 2.2 mm while the outer scale size L_o of the turbulence was taken to be 6.32 m. For the horizontal paths the constant in the structure function of the refractive index, C_n^2 was assumed to be $5 \times 10^{-14} m^{-2/3}$. This corresponds to the value obtained between 4:00 PM and 5:00 PM in Reference 10 and was here taken to represent moderate turbulence conditions. For the case of propagation through the total atmosphere, β represents the line-of-sight zenith angle.

It is worth noting that the value for m_G, the average value of G, given in Table 1 is extremely small for $\lambda = 0.63$ μm and the path length of 15 km. The precise numerical value of m_G given in the Table 1 for this case depends on the logarithm of G maintaining the normal distribution way out on the tails of the density function. It is doubtful whether this will be the case. As a result the accuracy of the value for m_G given for this case is seriously in question. Nevertheless this is of no consequence. The important result to note is that m_G/G can be expected to be much less than one. The low value for m_G/G for long distance propagation indicates the tendency for the signal amplitude as a function of time (when a constant sinusoid is transmitted) to take on the form of a spiked function for which $G \ll G_o$ most of the time with occassional spikes occurring where $G \gg G_o$.

Alternately, viewed from a spacial point of view, the received signal when projected on a screen will consist of a few bright spots in a grey background whose intensity is less than that which would exist if there were no turbulence.

The general expression for σ_1^2, the variance of the logarithm of the channel gain for a particular delay path, based on the assumptions of plane wave propagation along a path of constant C_n^2 is given by

$$\sigma_1^2 = 0.31\, C_n^2\, k^{7/6}\, L^{11/6} \qquad (2)$$

for $l_o \ll \sqrt{\lambda L} \ll L_o$ where L is the path length in meters and k is $2\pi/\lambda$ where λ is the wavelength of the radiation. For the case of propagation through the whole atmosphere

$$\sigma_1^2 = 0.5\, C_{no}^2\, k^{7/6}\, h_o^{3/2} (\sec \beta)^{11/6} \qquad (3)$$

where it is assumed here that C_n^2 varies with altitude h, in meters, as

$$C_n^2 = C_{no}^2\, h^{-1/3}\, e^{-h/h_o} \qquad (3a)$$

In Table 1, in order to make the conditions for the case of propagation through the whole atmosphere correspond to the former case, it was assumed that $h_o = 3200$ m and $C_{no}^2 = 1.83 \times 10^{-13}\ m^{-2/3}$. With these assumptions, as can be readily shown with (3a), $C_n^2 = 5 \times 10^{-14}\ m^{-2/3}$ at an altitude of 50 m. Table 2 gives the variation of C_n^2 with time of day. The results were based on data obtained at White Sands, New Mexico, over a 4 km path with an average elevation of about 140 feet for one particular day.[10] The time scale may shift for different days and will depend also on the season of the year, however, the general trend should remain the same. $C_n^2 = 5 \times 10^{-13}\ m^{-2/3}$ was taken to correspond to the case of strong turbulence. Equations (2) and (3) and the data in Table 2 permit one to obtain σ_1^2, σ_G^2 and m_G for other conditions than those used for obtaining Table I.

The time variable gain function $G(x_1, y_1, t)$ will not be independent of the time variable gain function $G(x_2, y_2, t)$ unless the distance between the points (x_1, y_1) and (x_2, y_2) is much greater than the transverse correlation distance at the receiving aperture. Figure 5 gives a plot of $R_G(\rho)$, the normalized spacial covariance function of the logarithm of the gain function, that is,

$$R_G(\rho) = \frac{\overline{\ln G(x_1, y_1; t)\ \ln G(x_2, y_2; t)}}{\left[\overline{\ln G(x, y; t)}\right]^2} \qquad (4)$$

where ρ is physically the separation between the points (x_1, y_1) and (x_2, y_2), i.e.

$$\rho = \sqrt{(x_1 - x_2)^2 + (y_1 - y_2)^2} \qquad (5)$$

The result in Figure 5 was obtained by assuming plane wave theory in which the turbulence is locally homogeneous.[11]

Based on theoretical analyses the time-variable delay function is expected to have a Gaussian distribution.[2] As in the case for the gains of the amplifiers for different scatter paths, the delays for different scatter paths are not independent unless their receiver elemental areas are separated by a sufficiently large amount. The spacial correlation function for the time delay function is given by

$$\tau^2(\rho) = \overline{\tau(x_1, y_1; t)\ \tau(x_2, y_2; t)} \qquad (6)$$

The channel dispersion is determined by the structure function of the time delay function given by

$$\tau_s^2(\rho) = \overline{\left[\tau(x_2, y_2; t) - \tau(x_1, y_1; t)\right]^2}$$

$$= 2\,\overline{\tau^2(o)} - 2\overline{\tau^2(\rho)} \qquad (7)$$

(Note from Reference 12 that $\tau_s^2(\rho) = D_\phi(\rho)/k^2c^2$, where $D_\phi(\rho)$ is the phase structure function, $k = 2\pi/\lambda$ is the wave number, and c is the speed of light.)

Table 3 tabulates $\tau_{rms}(\rho) \triangleq \sqrt{\tau_s^2(\rho)}$ and τ_{rms} ($\rho = L_o = 6.32$ m) for the frequencies and propagation paths given in Table 1. The same assumptions are made for corresponding propagation paths in Table 3 as were made in Table 1. The results are given in Table 3 for the assumption of plane wave propagation.

To obtain $\tau_{rms}(\rho)$ for other conditions than that given in Table 3 one uses the following general expression for $\tau_s^2(\rho)$ for the plane wave case

$$\tau_s^2(\rho) = 2.91 \frac{C_n^2}{c^2} L\, \rho^{5/3} \text{ for } \sqrt{\lambda L} \le \rho \le L_o \qquad (8)$$

$$\tau_s^2(\rho) = 1.49 \frac{C_n^2}{c^2} L\, \rho^{5/3} \text{ for}$$

$$\ell_o << \rho << \sqrt{\lambda L} \qquad (8a)$$

$$\tau_s^2(\rho) = 1.64 \frac{C_n^2}{c^2} \ell_o^{-1/3} L\rho^2 \text{ for}$$

$$\rho << \ell_o \qquad (8b)$$

where c is the velocity of light.[10,12] Equations (8), (8a) and (8b) hold for the assumption of plane wave propagation. For propagation through the whole atmosphere one uses the equation[12]

$$\tau_s^2(\rho) = 856 \frac{C_{no}^2}{c^2} \cdot \rho^{5/3} \text{ (sec } \beta) \qquad (8c)$$

It should be apparent from the above that if the receiver aperture is large enough to include a large number of scatter paths which are independent of each other and the outputs of the scatter paths of Figure 4 are added together using a heterodyning receiver, then when an unmodulated carrier is transmitted the amplitude of the detector instantaneous sum signal output will be a zero mean Gaussianly distributed signal as a result of the center limit theorem. Moreover, the detector output signal will be a Rayleigh fading signal, i.e., the envelope of the signal will be Rayleigh distributed and its phase uniformly distributed.

If a direct detector receiver system is utilized and a large receiver aperture is used such that many independent scatter paths are received, then again the detector signal will be Guassianly distributed, however, without zero mean. Moreover, in this case, the depth of the fading, or equivalently, the ratio of the r.m.s. to D.C. component of the signal, will decrease as the number of independent paths increases. The ratio of the root mean square value of the fluctuating component to the D.C. component for the detected signal will go down as one over the aperture diameter. This anticipated behavior is verified experimentally by the data given in Figure 6.[3,13] In effect the direct detector receiver system using a large aperture acts as a natural multiple diversity combining receiver for combating channel fading.

In the above, consideration was given to the ensemble average statistics of various channel parameters of interest. Now consideration will be given to the manner and rate with which the various channel parameters change. To determine the manner in which the amplitude of the signal changes with time, one makes use of Figure 5 which gives the nomalized spatial covariance function of the logarithm of the received signal amplitude. To determine the variation with time one makes the simple but reasonable approximation that the atmospheric inhomogenuities do not change with time except for a translational motion due to either the wind velocity or the movement of the incident ray

path across the atmosphere that would arise if one is observing the signal received from a moving transmitter, such as a low orbiting satellite. If one assumes a fixed transmitter, such as would be the case if it were located on a deep space vehicle, then one only has to contend with the wind velocity.

If the velocity normal to the ray path is v_n, then one has that the autocorrelation function of the fluctuations of the logarithmic amplitude with time are given by $R_G(v_n t)$. From Figure 5 the time for independence, τ_i, of the logarimthmic amplitude of the return signal at a point occurs when $v_n \tau_i \sqrt{\lambda L} = 0.76$. A typical wind velocity would be 5 m/sec. Thus for a path length through the atmosphere of 5 km, $\tau_i = 0.014$ sec. for $\lambda = 0.5$ μm. As a result the power spectrum of the logarimithmic amplitude variation is about 70 Hz wide for this case. These results agree favorably with measured values.[13,14] Figure 7 shows experimental fading data for the intensity of the received signal obtained from star data. The solid curve represents theoretical data on the signal intensity derived by Reiger.[13]

One can estimate the autocorrelation function of the propagation time for a particular path from which in turn the spectrum can be obtained by using equations (8) through (8c) and following a procedure similar to that discussed above for the obtaining the autocorrelation of the time variations of the logarithm of the return amplitude. By taking the Fourier Transform of the autocorrelation function of the propagation time one can theoretically obtain the power spectrum of the propagation time. However, obtaining the Fourier Transform of the autocorrelation function of the propagation time leads to unwieldy expressions.[12] Unfortunately little data is available for the power spectrum of the propagation time at laser frequencies. Until such data is available, though, one can obtain a direct estimate of the spectrum of the propagation time using the National Bureau of Standards data obtained at microwave frequencies.[15] Based on this data the power spectrum for the effective path length given in Figure 8 has been developed.[16] The model applies for 15 km atmospheric path length and a wind velocity perpendicular to the propagation path of 1 m/sec. Theoretically the index of refraction at laser frequencies will differ from that at microwave frequencies only by the contribution to the index of refraction provided by the water vapor in the air for microwave frequencies since the effects of the atmospheric water vapor on the index of refraction at laser frequencies is small in comparison. The difference in rms index of refraction variations for average humidity between microwave and laser frequencies is expected to be of the order of a factor of two.

Using the data of Figure 8 one finds that for propagation vertically through the whole atmosphere the coherence time at the laser wavelength of 0.69 μm is of the order of 10 ms.

Using the data of Figure 8 one can obtain the power spectrum for the angle of arrival of the incident beam, see Reference (16).

2. Inclement Weather Model

So far a model has been developed for good weather conditions. For inclement weather it is a little more difficult to specify precisely the model for the channel. In this case, particle scattering (due to the presence of fog, rain, snow, hail, or sleet) is very large and will determine the channel time dispersion. Figure 9 shows the multipathing that can arise from particle scattering during inclement weather. When particle scattering is large, no longer is the multipath time spread seen by a small receiving aperture negligible. More important, it can be considerably larger than the multipathing that arises when one uses a large receiving aperture under clear weather conditions. For a heavy fog condition, the dominant time dispersion will be due to the scattering from vapor particles. That this is the case has been shown theoretically and by experimental measurements by Chatterton.[8] The analysis that he made shows that the time dispersion is dependent on the field-of-view of the receiver aperture to a small degree and not on the size of the receiver aperture.

Specifically, a computer program which Chatterton carried out indicates that the risetime response, τ_r, of an optical signal propagating through a fog is

$\tau_r = 4.5\ \Delta t$ for $\theta_r = 4\alpha$,
the receiver wide-angle field-of-view case

and

$\tau_r = 3.3\ \Delta t$ for $\theta_r = \alpha/4$,
the receiver narrow-angle field-of-view case

where

$\Delta t = \alpha^2\, \ell / 2c$ nsec.

α = a forward-scatter angle (in radians) hypothesized for the scatterers in the fog

ℓ = mean path length in feet (it is physically the distance that the ray must travel to be attenuated by e^{-1})

c = velocity of light $\simeq 1$ foot/nsec

θ_r = the receiver field-of-view

The results indicate that the time dispersion for a 2.2 mile propagation path can be expected to be between 1 and 30 nanoseconds. The results are shown in Table 4. Chatterton's experimental data indicated a 2 nanosecond time dispersion for a length of 1.8 nautical miles. For the case where particle scattering is the dominant multipathing phenomena as in the case when a heavy fog is present, a suitable model for the channel is the

differential circuit model shown in Figure 10. The differential circuit model representation for the atmospheric channel, which is a linear time invariant channel, consists of a densely-tapped delay line with each tap being weighted by the function g (t, x) dx where g(t,x) is the Input Delay-Spread Function for the channel. Physically, g(t, x) dx is equal to the complex modulation produced by hypothetical element scatterers that provide delays in the range (x, x + dx). It remains to specify statistically the Input Delay-Spread Function for the channel.

Not dealt with in the above characterization of the channel is the channel noise. Consideration is given to the channel noise in Reference (17) also presented at the Fifth Space Congress.

3. Acknowledgement

The author has benefited immensely from innumerable discussions with Professor E.V. Hoversten of the Massachusetts Institute of Technology. Table 1 and 3 are based on tables originally prepared by Professor Hoversten. The author is also indebted to Dr.P. Miles of the Raytheon Company Research Division for his comments. Finally, thanks are due to the Project Leader, Mr. A. Jelalian for his encouragement during the course of the study for which the major part of this work was performed.

4. References

1. Muchmore, R.B., and Wheelon, A.D., "Frequency Correlation of Line-of-Sight Signal Scintillations", IEEE Transactions on Antennas and Propagation, Vol. AP-11, No. 1, January 1963, pp. 46-51.

2. Hoversten, E.V., "The Atmosphere as an Optical Communication Channel", IEEE International Convention Record, Part 2, March 20, 21, 23, 1967, pp. 137-145.

3. Ellison, M.A., and Seddon, H., "Some Experiments on the Scintillation of Stars and Planets", Monthly Notices of the Royal Astronomical Society, Vol. 112, 1952, pp. 73-87.

4. Born, M. and Wolf, E. "Principles of Optics", McGraw-Hill Book Company, New York, 1964.

5. Brookner, E., "Effect of Ionosphere on Radar Waveforms", Journal of the Franklin Institute, vol. 280, July, 1965, pp. 1-22.

6. Long, R. K., "Absorption at Ruby Laser Wavelengths for Low Angle Total Atmospheric Paths", Technical Report 2156-2, Antenna Laboratory, Ohio State University Research Foundation, Columbus, Ohio, 31 December, 1966.

7. Long, R. K., "Absorption of Laser Radiation in the Atmosphere", Technical Report 1579-3, Antenna Laboratory, Ohio State University Research Foundation, Columbus, Ohio, May 31, 1963,

8. Chatterton, E. G., "Optical Communications Employing Semiconductor Lasers", Technical Report 392, Lincoln Laboratory, Massachusetts Institute of Technology, June 9, 1965.

9. Bello, P. A., "Characterization of Randomly Time-Varient Linear Channels", IEEE Transaction of Communications Systems, Vol. CS-11, December, 1963, pp. 360-393.

10. Goldstein, I., Miles, P.A., and Chabot, A., "Heterodyne Measurements of Light Propagation through Atmospheric Turbulence", Proc. of IEEE, Vol, 53, No. 9, September 1965, pp. 1172-1180.

11. Tatarski, V. I., "Wave Propagation in a Turbulent Medium" (translated by R. A. Silverman), McGraw-Hill Book Company, New York, 1961.

12. "Laser Communications" Final Report, Report No. U67-4038, Space and Information Division, Raytheon Company, Sudbury, Massachusetts, December 31, 1966.

13. Reiger, S. H., "Starlight Scintillation and Atmospheric Turbulence", Astronomical Journal, Vol. 68, August, 1963, pp. 395-406.

14. Mikesell, A. H., "The Scintillation of Starlight", U.S. Naval Observatory, Washington, D.C.

15. Thompson, M. C., James, H. B., and Kirkpatrick, R. W., "An Analysis of Time Variations in Tropospheric Refractive Index and Apparent Radio Path Length", Journal of Geophysical Research, Vol. 65, January, 1960, pp. 193-201.

16. Unger, J. H. W., "Random Tropospheric Angle Errors in Microwave Observations of the Early Bird Satellite", The Bell System Technical Journal, Vol. 45, November 1966, pp. 1439-1472.

17. Brookner, E., "Performance of Single and Multiple-Dish Laser Communication Systems", Fifth Space Congress, Cocoa Beach Florida, March 11-14, 1968.

TABLE 1

Path Gain Variances in Clear Weather Model

Path Length	0.63 μ	10.6 μ
1 km	$\sigma_1^2 = 0.71$ $\sigma_G^2 = 0.506\ G_o^2$ $m_G = 0.7\ G_o$	$\sigma_1^2 = 2.65 \times 10^{-2}$ $\sigma_G^2 = 2.65 \times 10^{-2}\ G_o^2$ $m_G = 0.987\ G_o$
15 km	$\sigma_1^2 = 1.0 \times 10^2$ $\sigma_G^2 = G_o^2$ $m_G = 5 \times 10^{-21}\ G_o$	$\sigma_1^2 = 3.8$ $\sigma_G^2 = 0.978\ G_o^2$ $m_G = 0.15\ G_o$
Total Atmosphere	$\sigma_1^2 = 2.42\ (\sec \beta)^{11/6}$ For $\beta = 0$ $\sigma_G^2 = 0.911\ G_o^2$ $m_G = 0.289\ G_o$	$\sigma_1^2 = 9.0 \times 10^{-2} (\sec \beta)^{11/6}$ For $\beta = 0$ $\sigma_G^2 = 9.1 \times 10^{-2}\ G_o^2$ $m_G = 0.956\ G_o$

Where: σ_1^2 = Variance of $\ln G/G_o$

$\sigma_G^2 = \overline{(G - \bar{G})^2} = G_o^2 \left[1 - \exp\left(-\sigma_1^2\right)\right]$

$m_G = \bar{G} = G_o \exp\left(-\frac{1}{2}\sigma_1^2\right)$

TABLE 2

C_n^2 Versus Time of Day

Time	C_n^2 (Meter)$^{-2/3}$
1200	5×10^{-14}
1300	1.4×10^{-13}
1400	4.9×10^{-13}
1500	1.4×10^{-13}
1600	2×10^{-14}
1700	5×10^{-15}
1800	5×10^{-16}
1900	small
2000	5×10^{-16}
2100	2×10^{-15}
2200	3×10^{-15}
2300	5×10^{-15}

Time	C_n^2 (Meter)$^{-2/3}$
2400	8×10^{-15}
0100	↑
0200	↓
0300	$< 10^{-14}$
0400	↑
0500	
0600	
0700	
0800	
0900	$< 5 \times 10^{-14}$
1000	↓
1100	

TABLE 3

Time Delay

Path Length	Plane Wave Transmission	
	General Expression*	τ_{rms} ($\rho = L_o = 6.32$ m)
1 km	$\tau_{rms}(\rho) = 3.9 \times 10^{-14}\ \rho^{5/6}$ for $6.32\text{ m} \geq \rho \geq 2.5$ cm when $\lambda = 0.63\mu$ and for $6.32\text{ m} \geq \rho \geq 10$ cm when $\lambda = 10.6\mu$ $\tau_{rms}(\rho) = 2.76 \times 10^{-14}\ \rho^{5/6}$ for 2.2 mm $\leq \rho \leq 2.5$ cm when $\lambda = 0.63\mu$ and for 2.2 mm $\leq \rho \leq 10$ cm when $\lambda = 10.6\mu$	0.18 picosec.
15 km	$\tau_{rms}(\rho) = 1.5 \times 10^{-13}\rho^{5/6}$ for $6.32\text{ m} \geq \rho \geq 9.7$ cm when $\lambda = 0.63\mu$ and for $6.32\text{ m} \geq \rho \geq 39$ cm when $\lambda = 10.6\mu$ $\tau_{rms}(\rho) = 1.06 \times 10^{-13}\rho^{5/6}$ for 2.2 mm $\leq \rho \leq 9.7$ cm when $\lambda = 0.63\mu$ and for 2.2 mm $\leq \rho \leq 39$ cm when $\lambda = 10.6\mu$	0.70 picosec.
Total Atmosphere	$\tau_{rms}(\rho) = 4.2 \times 10^{-14}\rho^{5/6}\ (\sec\beta)^{1/2}$ for $\rho \geq 2.6$ cm when $\lambda = 0.63\mu$ and for $\rho \geq 11$ cm when $\lambda = 10.6\mu$ $\tau_{rms}(\rho) = 2.97 \times 10^{-14}\rho^{5/6}\ (\sec\beta)^{1/2}$ for 2.2 mm $\leq \rho \leq 2.6$ cm when $\lambda = 0.63\mu$ and for 2.2 mm $\leq \rho \leq 11$ cm when $\lambda = 10.6\mu$	0.19 picosec.

*NOTE: $\tau_{rms}(\rho)$ is in seconds and ρ is in meters.

TABLE 4

Channel Risetime, τ_r (in nanoseconds)

Under Conditions of Fog

Path Length	$L = 7\ell$	$L = 7\ell$ = 2.2 miles = 4.4 km	
α	α	1^o	5^o
Wide-Angle System ($\theta_r = 4\alpha$)	$\tau_r = 4.5\ \Delta t$	1.1	29
Narrow-Angle System ($\theta_r = \alpha/4$)	$\tau_r = 3.3\ \Delta t$	0.8	21

NOTE: $\Delta t \triangleq \frac{\alpha^2 \ell}{2c}$

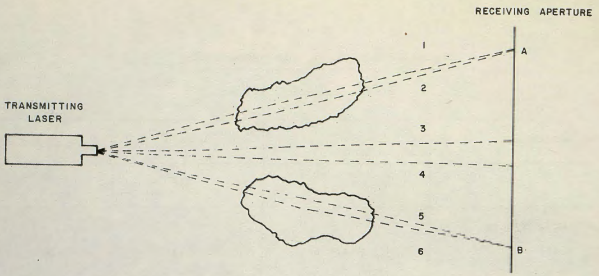

(1) Multipathing Due to Atmospheric Turbulence for the Case of Clear Weather

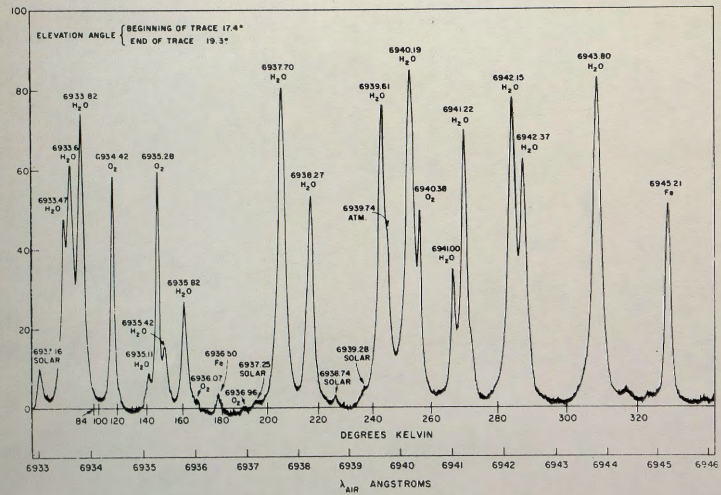

(2) Atmospheric Absorption of the Ruby Laser Wavelength

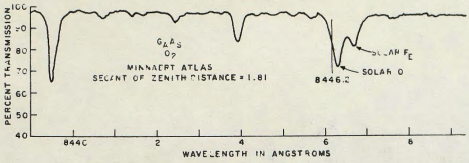

(3) Atmospheric Absorption Near the GaAs Wavelength of 8446.2 Å

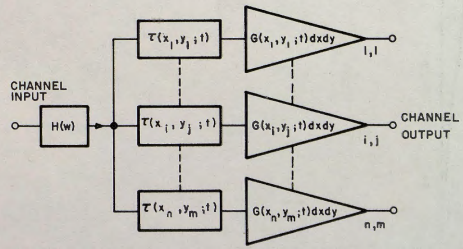

(4) Clear Weather Circuit Model of the Dispersive Atmospheric Channel

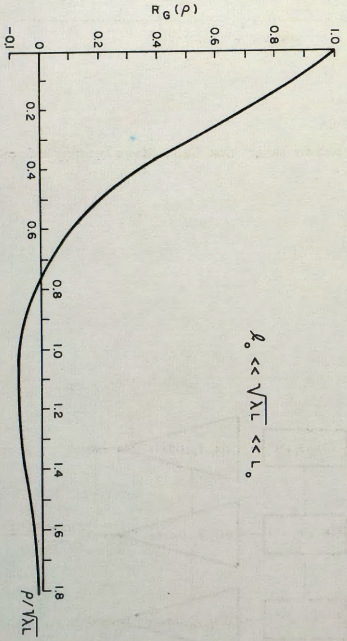

(5) Normalized Spacial Covariance Function of the Logarithmic Amplitude of the Field After Propagation over a Path of Length L

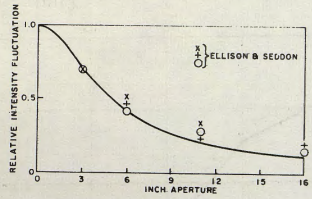

(6) Scintillation vs. Telescope Aperture

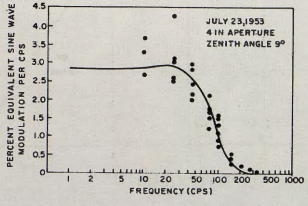

(7) Intensity Spectrum for 4-inch Aperture

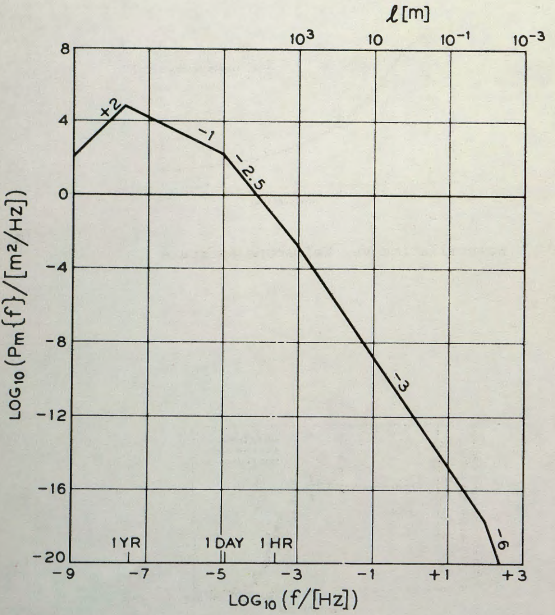

(8) Model Power Density Spectrum $P_m\{f\}$ of Tropospheric Random Errors in the Range Coordinate Versus Error-Frequency, f, in a Log-Log Plot. The Tropospheric Anomalies have the Characteristic Length ℓ given in Meters on the Top Scale

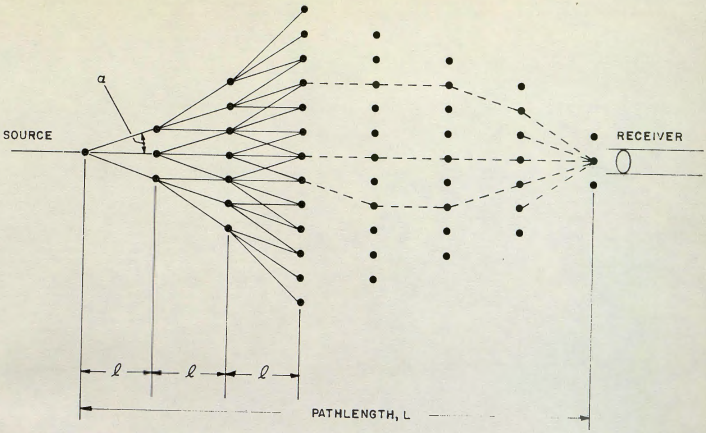

(9) Multiple-Scatter Path Model for the Case of Inclement Weather

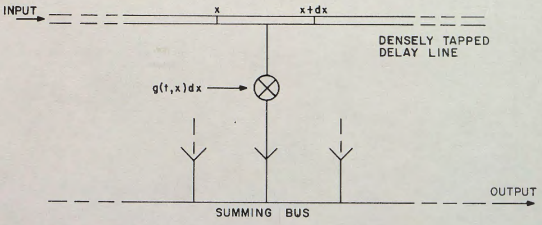

(10) Inclement Weather Differential Circuit Model of Dispersive Atmospheric Channel